

Supporting Information

True Photoreactivity Origin of Ti^{3+} -Doped Anatase TiO_2 Crystals with Respectively Dominated Exposed $\{001\}$, $\{101\}$ and $\{100\}$ Facets

Xiaogang Liu,^{*a} Guiru Du ^a and Meng Li ^b

a. College of Chemistry and Chemical Engineering, Xinyang Normal University,

Xinyang, Henan 464000, P. R. China.

b. Business School, Xinyang Normal University, Xinyang, Henan 464000, P. R.

China.

Additional figures and tables.

Table S1. Average exposed percentages of {001}, {101} and {100} facet in R-TiO₂-001, R-TiO₂-101 and R-TiO₂-101, calculated from the surface areas of each facet from SEM and TEM images.

Sample	{001}	{101}	{100}
R-TiO ₂ -001	82%	18%	0
R-TiO ₂ -101	14%	86%	0
R-TiO ₂ -100	4%	12%	84%

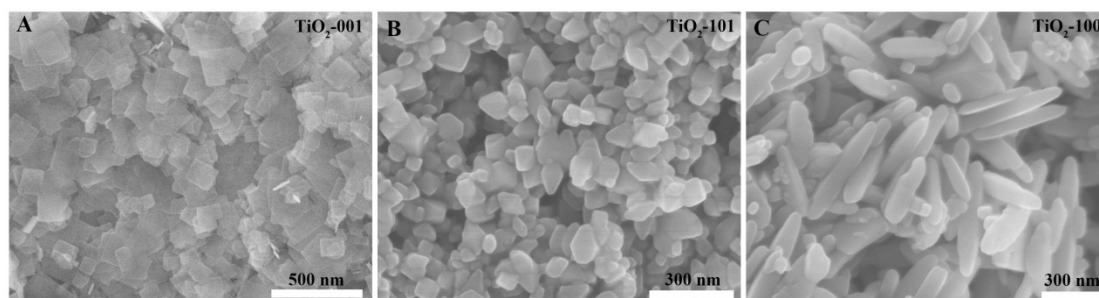


Figure S1. SEM images of TiO₂ samples with different dominant facets: A) TiO₂-001; B) TiO₂-101 and C) TiO₂-100.

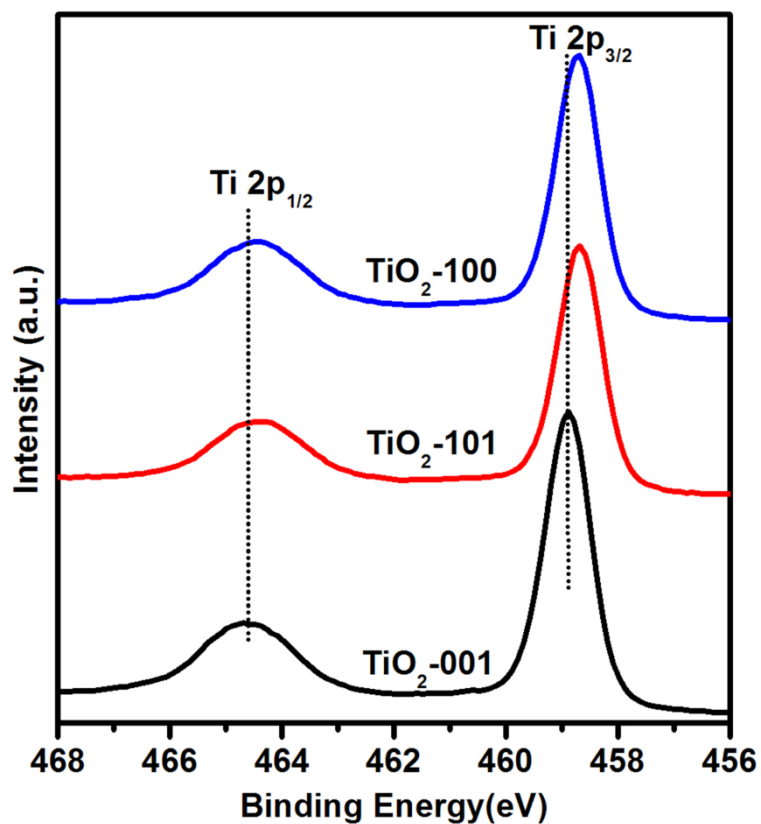


Figure S2. XPS spectra of Ti 2p for TiO₂ with different predominated exposed facets before Al reduction.

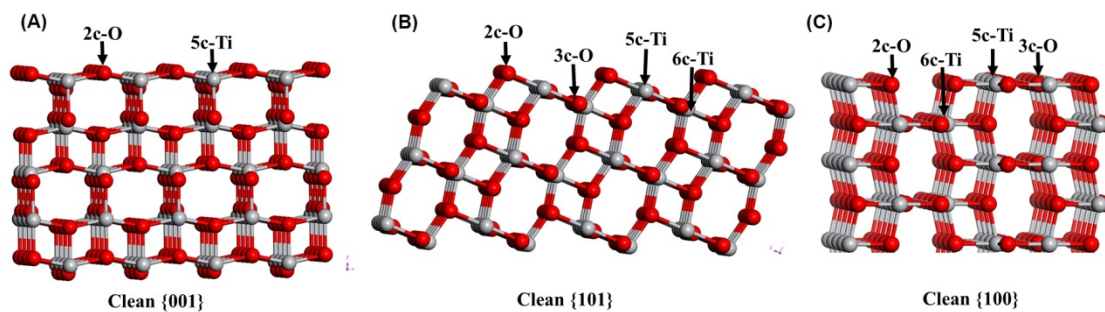


Figure S3. Schematic of atomic surface structure of anatase TiO_2 with (A) clean $\{001\}$, (B) clean $\{101\}$ and (C) clean $\{100\}$ facets.

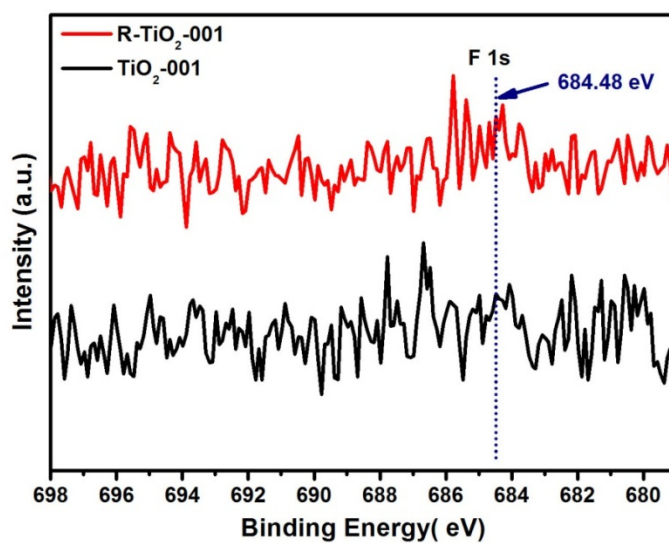


Figure S4. The F 1s XPS spectra of R- TiO_2 -001 and TiO_2 -001 sample.

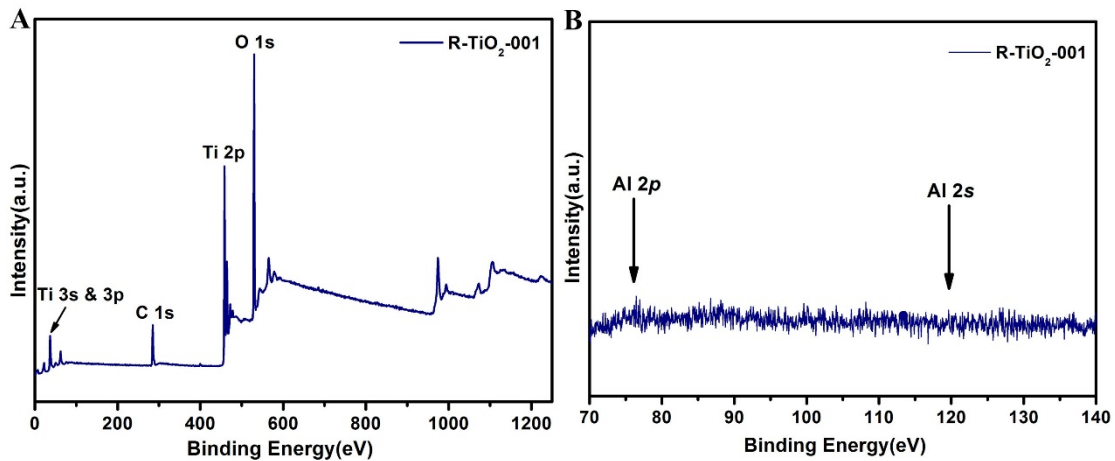


Figure S5. XPS survey spectra (A) and Al element analysis (B) of of R-TiO₂-001 sample.

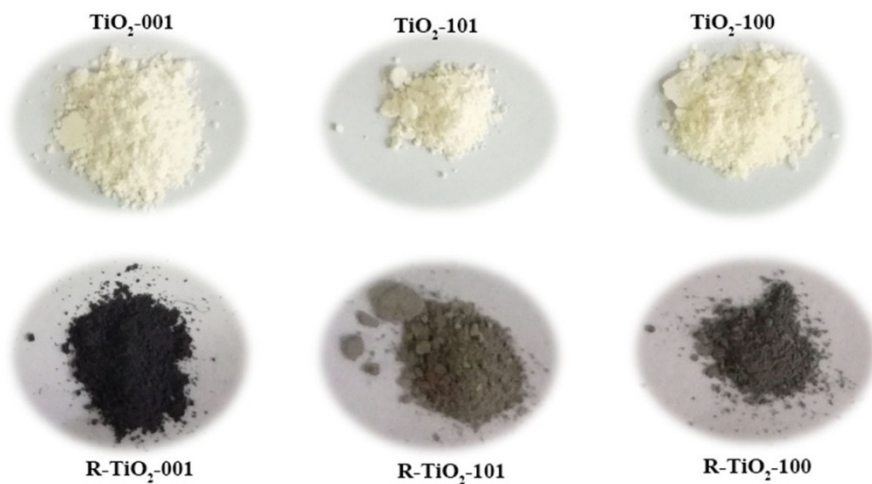


Figure S6. The digital photography of prepared TiO₂ samples before and after Al reduction.

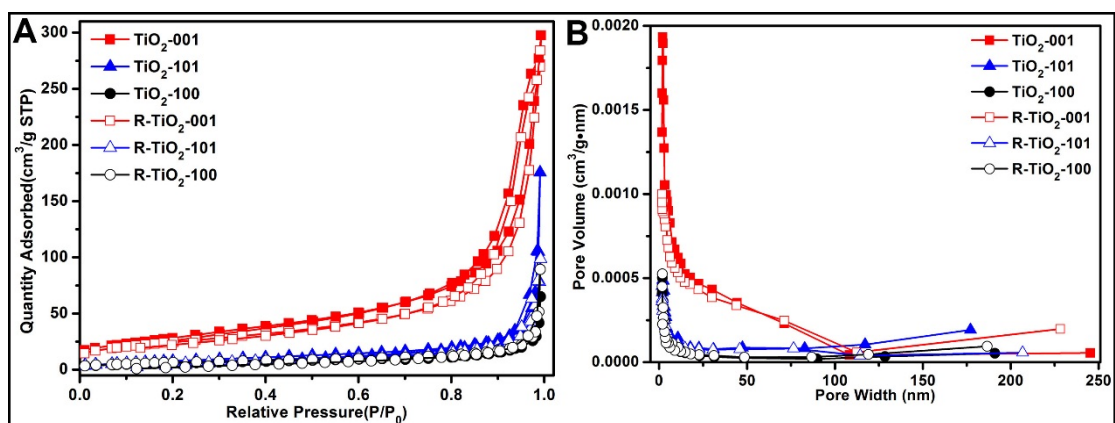


Figure S7. N₂ adsorption-desorption isotherm (A) and pore size distribution (B) of prepared TiO₂ nanocrystals before and after Al reduction.

Table S2. BET surface areas and pore parameters of prepared TiO₂ samples before and after Al reduction.

Samples	S _{BET} (cm ² /g)	Pore Volume(cm ³ /g)	Pore Size(nm)
TiO ₂ -001	25.1059	0.044919	7.38264
R-TiO ₂ -001	21.7914	0.040023	7.34654
TiO ₂ -101	31.7491	0.084714	10.67288
R-TiO ₂ -101	24.3378	0.066210	10.54896
TiO ₂ -100	103.7212	0.310701	11.98215
R-TiO ₂ -100	99.5281	0.274669	12.27187

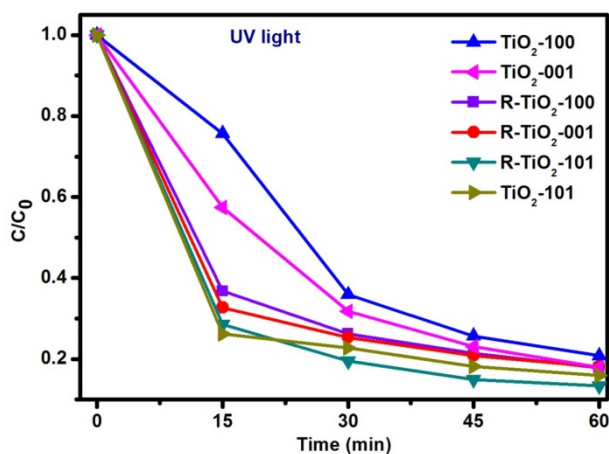


Figure S8. The degradation curves of phenol over different photocatalysts under ultraviolet-light irradiation..

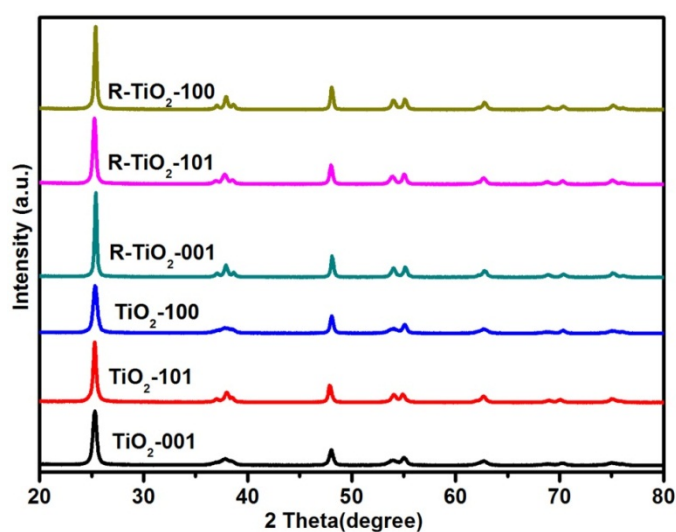


Figure S9. Re-tested XRD patterns for TiO₂ and reduced TiO₂ nanocrystals after photocatalytic performance evaluation.

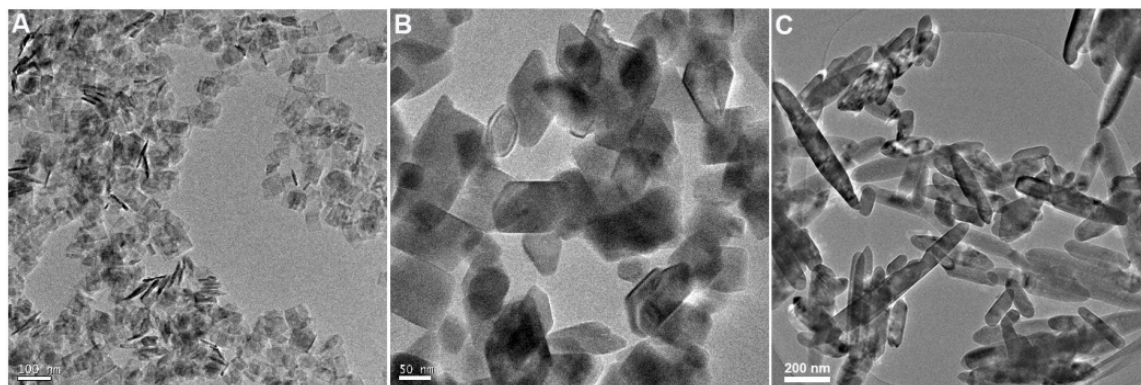


Figure S10. TEM images of (A) R-TiO₂-001, (B) R-TiO₂-101 and (C) R-TiO₂-100 after photocatalytic performance tests.

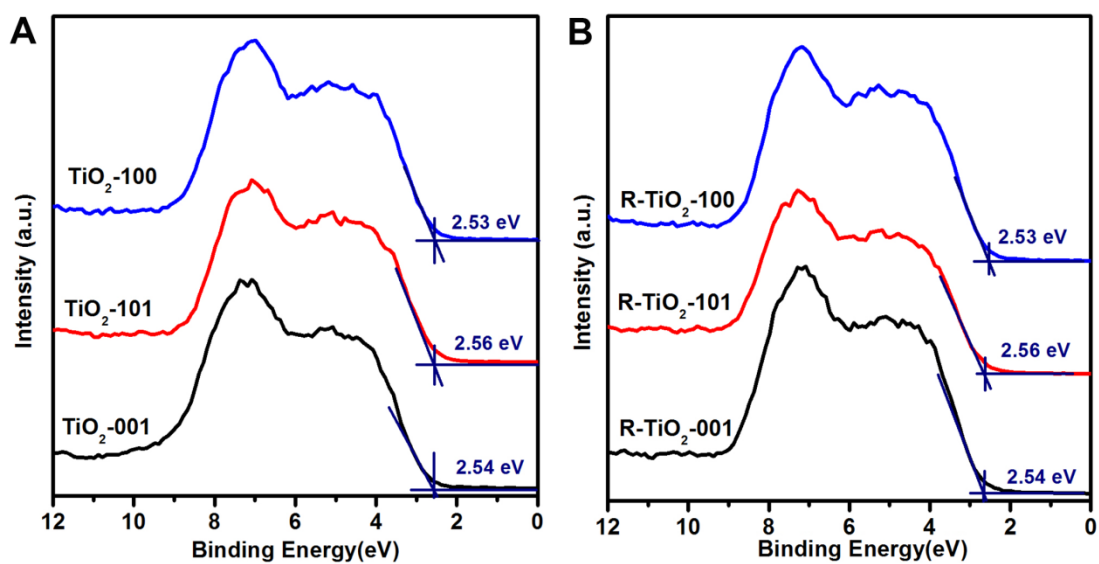


Figure S11. XPS valence band spectrum of as prepared TiO₂ with different dominant exposed facets before (A) and after (B) Ti³⁺ doping.

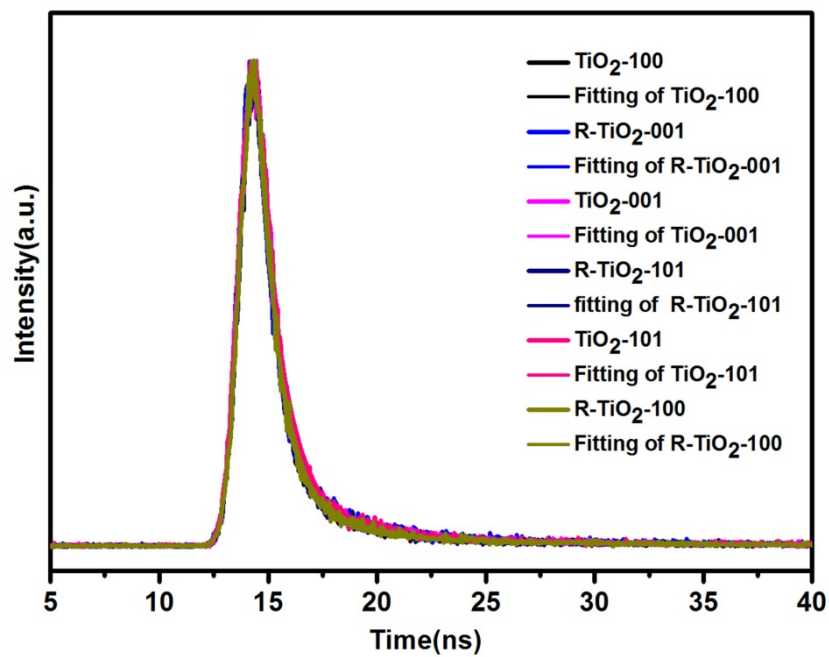


Figure S12. Time-resolved fluorescence decay spectra of prepared TiO₂ samples.